

# Nonlocal Topological Maxwell Demon Teleporting Ergotropy via Surface-Code Quantum Error Correction

M. Y. Abd-Rabbou<sup>1,\*</sup> and Cong-Feng Qiao<sup>1,2,†</sup>

<sup>1</sup>*School of Physics, University of Chinese Academy of Sciences, Yuquan Road 19A, Beijing, 100049, China.*

<sup>2</sup>*International Centre for Theoretical Physics Asia-Pacific, UCAS, Beijing 100190, China.*

We introduce a nonlocal Maxwell demon teleporting ergotropy at finite temperature via classical communication and a shared surface code. The teleported ergotropy is exponentially protected below a topological threshold. We identify a thermodynamic phase transition separating a profitable demon phase from a thermal phase. A quadratic infrastructure cost strictly enforces the second law, imposing a fundamental thermodynamic horizon on separation distance. This establishes quantum error correction as a resource for nonlocal thermodynamics beyond fault-tolerant computation.

Landauer’s erasure principle establishes that erasing one bit of information from a demon’s memory dissipates at least  $k_B T \ln 2$  of heat into the environment [1, 2], resolving the apparent paradox posed by Maxwell’s demon [3]. This bound has been confirmed experimentally in both classical [4] and quantum [5, 6] systems, and the Sagawa-Ueda bound quantifies precisely how much work an informed agent can extract from a single measurement outcome [7]. In all such realisations, the measurement and the work extraction occur at the same spatial location.

A natural extension is to spatially separate the two operations: one party measures a quantum system and transmits a classical record to a distant party who performs the work extraction. Quantum energy teleportation (QET) achieves energy transfer of this type using only local operations and classical communication, with a shared entangled ground state providing the correlations [8–11]. However, QET operates near absolute zero, where the ground-state correlations are intact; at finite temperature these correlations degrade and the protocol fails. Moreover, QET transfers bare internal energy, which need not be convertible into work. The relevant figure of merit for a quantum work-storage device is the ergotropy [12], defined as the maximum work extractable by unitary operations, which serves as the operationally meaningful measure of stored energy in quantum batteries [13–15]. Whether ergotropy can be transferred nonlocally at finite temperature, in a thermodynamically consistent manner, has remained an open question.

Surface-code quantum error correction provides a mechanism to actively maintain a logical qubit against thermal noise [16–18]. Recent experiments have demonstrated logical error rates below the physical threshold on superconducting processors [19–21], establishing that topologically ordered states are experimentally accessible at finite temperature. Crucially, the teleportation of a surface-code logical qubit has recently been demon-

strated locally on a single processor [22]. This establishes the technological foundation for our work, which investigates the thermodynamic limits of extending such teleportation across macroscopic distances.

This Letter introduces an ergotropy teleportation protocol in which a surface code serves as the thermodynamic channel between two separated parties. Rather than physically transmitting energy through the code’s degenerate ground space, Alice expends ergotropy  $\Delta E$  from her local battery to drive the logical-qubit charging interaction  $H_{\text{int}}(t) = g(t)\sigma_A^x \otimes \bar{Z}_L$ . She then transmits the classical syndrome record  $\vec{s}_A$  to Bob. This classical information acts as an entropy rectifier [7]. Without  $\vec{s}_A$ , Bob’s conditional unitary is applied at random relative to the true logical state and no ergotropy is recovered. With  $\vec{s}_A$ , Bob decodes the logical state via minimum-weight perfect matching and conditionally charges his battery, storing ergotropy  $\mathcal{E}_B = (2P_{\text{succ}} - 1)\Delta E$ . The five-stage protocol is illustrated schematically in Fig. 1. Three results follow from this construction. Below a topological threshold  $p_{\text{th}}$ , the logical error rate  $P_{\text{log}}$  is exponentially suppressed in code distance, so that  $P_{\text{succ}} \rightarrow 1$  exponentially and efficient transfer becomes possible. A thermodynamic phase transition at a critical error rate  $p_c$ , which exceeds  $p_{\text{th}}$ , separates a profitable regime from a thermal regime in which costs dominate. The second law is strictly satisfied at all separations. A quadratic infrastructure cost imposes a fundamental thermodynamic horizon  $N_{\text{max}} \propto \sqrt{\Delta E/\varepsilon_m}$  beyond which the protocol cannot operate profitably, independent of code distance or decoder quality.

*Model and Protocol*— We consider a rotated surface code on a rectangular lattice  $\Lambda = \{(x, y) \in \mathbb{Z}^2 \mid 0 \leq x \leq N, 0 \leq y \leq L\}$ , where  $L$  is the code distance and  $N \gg L$  is the separation between Alice ( $x = 0$ ) and Bob ( $x = N$ ). Physical qubits reside on the edges of  $\Lambda$ , with total count  $|E| = 2NL + N + L$  (Supplemental Material, Sec. I). The system is governed by the stabiliser Hamiltonian [16, 17]

$$H_{\text{SC}} = -J \sum_{v \in V} A_v - J \sum_{p \in P} B_p, \quad J > 0, \quad (1)$$

where  $A_v = \prod_{j \in \text{star}(v)} \sigma_j^x$  and  $B_p = \prod_{j \in \partial p} \sigma_j^z$ . All sta-

\* m.elmalky@azhar.edu.eg

† qiaocf@ucas.ac.cn

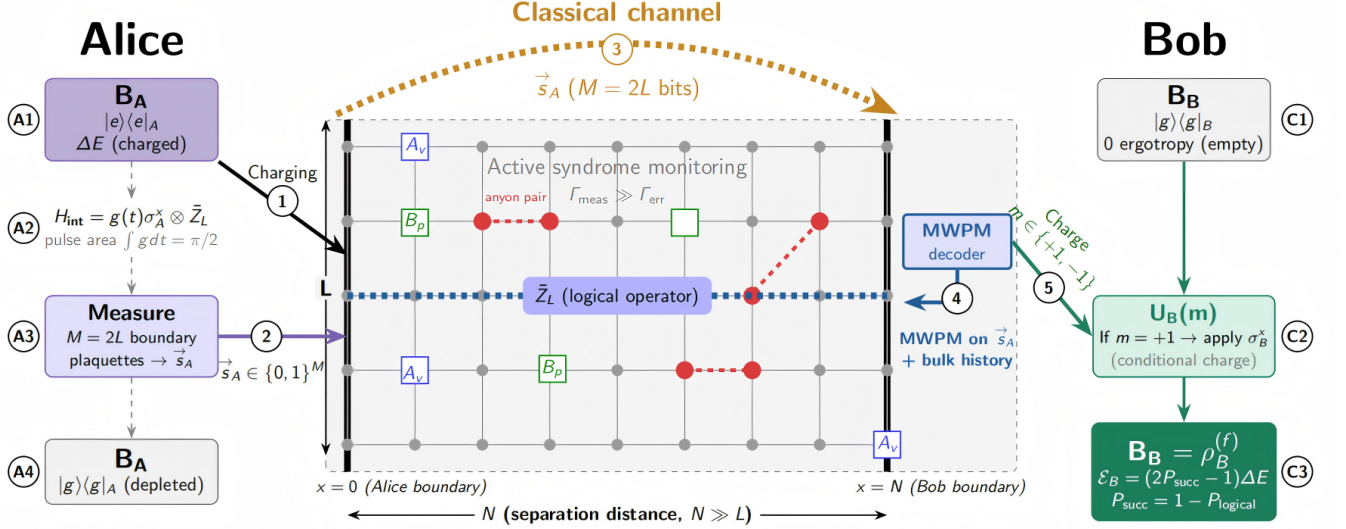


FIG. 1. Five-stage ergotropy teleportation protocol. Purple: Alice operations; teal: Bob operations; blue dashed: logical operator  $\bar{Z}_L$ ; amber dashed: classical channel; red: thermally excited anyon pairs. Alice charges the logical qubit (stage (1)), measures  $M = 2L$  boundary plaquettes (stage (2)), and transmits  $\vec{s}_A$  to Bob (stage (3)). Bob decodes via minimum-weight perfect matching (stage (4)) and conditionally charges his battery (stage (5)), extracting ergotropy  $\mathcal{E}_B = (2P_{\text{succ}} - 1)\Delta E$  with energy balance  $\Delta E + W_{\text{ops}} + W_{\text{bulk}} = \mathcal{E}_B + Q_{\text{diss}}$  (Eq. 6).

bilisers commute since any vertex and plaquette share zero or two edges, and the ground state manifold encodes one logical qubit. The logical operator  $\bar{Z}_L = \prod_{j \in \gamma} \sigma_j^z$  runs along any horizontal path  $\gamma$  from Alice to Bob; path independence on code states is proved in Sec. I of the Supplemental Material. Thermal fluctuations at temperature  $T$  excite anyon pairs with probability  $p \approx \exp(-4J/k_B T)$ , giving  $T = -4J/(k_B \ln p)$ . Without active monitoring, topological order in two dimensions is unstable at any finite  $T$  [17]. Anyons diffuse and produce logical errors on a timescale independent of  $N$ , causing the stored ergotropy to vanish.

The protocol proceeds in five stages (Fig. 1). Alice holds a battery  $\mathcal{B}_A$  with Hamiltonian  $H_A = (\Delta E/2)\sigma_A^x$ , initially fully charged,  $\rho_A^{(0)} = |e\rangle\langle e|_A$ . Bob's battery is identical but initially empty,  $\rho_B^{(0)} = |g\rangle\langle g|_B$ . In Stage 1, Alice applies the interaction  $H_{\text{int}}(t) = g(t)\sigma_A^x \otimes \bar{Z}_L$  with pulse area  $\int g dt = \pi/2$ , expending energy  $\Delta E$  from her battery to drive the logical state encoding, leaving  $\rho_A^{(1)} = |g\rangle\langle g|_A$ . The corresponding evolution operator

$$U_{\text{charge}} = \exp\left(-\frac{i\pi}{2}\sigma_A^x \otimes \bar{Z}_L\right) = -i\sigma_A^x \otimes \bar{Z}_L \quad (2)$$

satisfies  $[\bar{Z}_L, H_{\text{SC}}] = 0$ , so the code stabiliser energy is unchanged; the energy  $\Delta E$  is encoded in the logical-qubit degree of freedom. Crucially, owing to the path independence of logical operators on the code space, Alice intentionally applies the specific string representative of  $\bar{Z}_L$  that lies entirely along her boundary at  $x = 0$ . This guarantees her physical operation is strictly local, preserving the LOCC nature of the protocol. The extended

string operator spanning the lattice emerges only computationally when Bob performs global minimum-weight perfect matching. This guarantees that no physical energy or operations cross the channel. The derivation of the pulse condition and the full density matrix evolution are given in Sec. II of the Supplemental Material. In Stage 2, Alice measures  $M = 2L$  boundary stabilisers ( $L$  of  $X$ -type and  $L$  of  $Z$ -type along the  $x = 0$  edge), recording  $\vec{s}_A \in \{0, 1\}^M$ . In Stage 3, she transmits  $\vec{s}_A$  to Bob via a classical channel. This is the sole communication between the two parties. In Stage 4, Bob applies minimum-weight perfect matching [17, 23] to  $\vec{s}_A$  and the bulk syndrome history, obtaining correction  $m \in \{+1, -1\}$ . In Stage 5, Bob applies  $U_B(m) = \sigma_B^x$  conditionally on  $m = +1$ , charging his battery.

The ergotropy of Bob's battery after the cycle follows from the passive-state construction [12]; the complete four-step derivation is given in Sec. III of the Supplemental Material. With final state  $P_{\text{succ}}|e\rangle\langle e|_B + (1 - P_{\text{succ}})|g\rangle\langle g|_B$ , the result is

$$\mathcal{E}_B = (2P_{\text{succ}} - 1)\Delta E, \quad (3)$$

where  $P_{\text{succ}} = 1 - P_{\text{log}}$  is the MWPM decoding success probability.

Crucially, active syndrome monitoring over  $R$  rounds exponentially suppresses logical errors below the topological threshold  $p_{\text{th}}$ , yielding

$$P_{\text{succ}} \approx 1 - (N \cdot R) A \left(\frac{p}{p_{\text{th}}}\right)^{(L+1)/2}, \quad (4)$$

where  $A$  is a geometry-dependent prefactor and  $(N \cdot R)$

is the spacetime volume. Causality requires Alice's syndrome record to reach Bob before decoding, forcing  $R \geq N/c_{\text{signal}}$  (where  $c_{\text{signal}}$  is the physical speed of the classical channel), so the spacetime volume scales as  $N \cdot R \propto N^2$ . Substituting into Eq. (4), the logical error rate grows quadratically with separation at fixed  $p$  and  $L$ ; this is the kinematic origin of the  $N^2$  infrastructure cost derived below.

The Sagawa-Ueda bound [7] on extracted ergotropy gives

$$\mathcal{E}_B \leq k_B T I(E : \vec{s}_A) \leq M k_B T \ln 2, \quad (5)$$

where the second inequality saturates when  $\vec{s}_A$  is maximally informative. This bound is never violated by our protocol (proof in Sec. IV of the Supplemental Material). Eq. (3) vanishes at  $P_{\text{succ}} = \frac{1}{2}$  (random guessing, no information) and reaches  $\Delta E$  at  $P_{\text{succ}} = 1$  (perfect decoding). The classical syndrome  $\vec{s}_A$  acts as an entropy rectifier. It converts Bob's local energy into ergotropy without any direct physical energy flow through the channel.

*Thermodynamic Analysis.*— The protocol draws on three independent work inputs: Alice's battery contributes  $\Delta E$  to drive the Stage-1 logical encoding; external erasure apparatus supplies  $W_{\text{ops}}$ ; and external syndrome-measurement apparatus supplies  $W_{\text{bulk}}$ . Neither  $W_{\text{ops}}$  nor  $W_{\text{bulk}}$  is drawn from Alice's battery (see Supplemental Material Sec. IV). The exact energy conservation law is

$$\Delta E + W_{\text{ops}} + W_{\text{bulk}} = \mathcal{E}_B + Q_{\text{diss}}, \quad (6)$$

where  $W_{\text{ops}} \approx 2Mk_B T \ln 2$  ( $M = 2L$ ) is the Landauer cost of erasing the syndrome register [1, 2], and  $Q_{\text{diss}} \geq 0$  is heat dissipated by imperfect decoding. The infrastructure cost is derived from the active spacetime volume. Sustaining  $2LN$  stabilisers over  $R$  syndrome rounds costs  $\varepsilon_m$  per stabiliser-round, giving  $W_{\text{bulk}} = (2LN) \cdot R \cdot \varepsilon_m$ . As established, causality enforces  $R \geq \frac{N/c_{\text{signal}}}{\tau_m}$ , yielding  $R \approx R_0 N$  (where  $R_0 = 1/(c_{\text{signal}}\tau_m)$  is the minimum syndrome rounds per unit separation required by causality,  $c_{\text{signal}}$  is the classical communication speed, and  $\tau_m$  is the duration of one syndrome cycle). Because the channel has width  $L$ , the active spacetime volume is proportional to  $L \cdot N^2$ , making the infrastructure cost grow quadratically as

$$W_{\text{bulk}} = 2LR_0 \varepsilon_m N^2. \quad (7)$$

The net transferred ergotropy is  $W_{\text{net}} = \mathcal{E}_B - W_{\text{ops}} - W_{\text{bulk}}$ .

Using the Sagawa-Ueda bound Eq. (5),  $\mathcal{E}_B \leq W_{\text{ops}}$ . This, combined with the strictly positive  $W_{\text{bulk}}$ , guarantees that the total entropy production satisfies

$$\Delta S_{\text{total}} = \frac{Q_{\text{bath}}}{T} + \Delta S_{\mathcal{B}_B} \geq \frac{\Delta E + W_{\text{bulk}} - \mathcal{E}_B}{T} \geq \frac{W_{\text{bulk}}}{T}, \quad (8)$$

where  $Q_{\text{bath}} = \Delta E + W_{\text{ops}} + W_{\text{bulk}} - \mathcal{E}_B \geq W_{\text{bulk}} > 0$  and  $\Delta S_{\mathcal{B}_B} \geq 0$ , yielding

$$\Delta S_{\text{total}} \geq \frac{W_{\text{bulk}}}{T} > 0 \quad (9)$$

for all  $N > 0$ : the demon never violates the second law because maintaining the topological channel always dissipates entropy into the bath, regardless of how well the decoding performs (proof in Supplemental Material Sec. IV).

The quadratic growth of  $W_{\text{bulk}}$  against the nearly distance-independent  $\mathcal{E}_B$  creates a fundamental limit on profitable operation. Setting  $W_{\text{net}} = 0$  gives the thermodynamic horizon

$$N_{\text{max}} = \sqrt{\frac{(2P_{\text{succ}} - 1) \Delta E - 2Mk_B T \ln 2}{2LR_0 \varepsilon_m}}, \quad (10)$$

beyond which the channel costs more to maintain than it delivers. Notably, both the battery capacity  $\Delta E$  and the classical syndrome bandwidth  $M = 2L$  scale linearly with the code distance  $L$ . Consequently, the variable  $L$  completely cancels out of the fraction. Thus,  $N_{\text{max}}$  is strictly independent of the code distance: once  $L$  is large enough that  $P_{\text{succ}} \approx 1$  below threshold, the horizon is bounded entirely by the ratio of energy density to measurement cost.

Similarly, the thermodynamic critical error rate  $p_c$ , at which  $W_{\text{net}} = 0$  at fixed  $N$ , is determined implicitly by balancing linear density terms

$$(2P_{\text{succ}}(p_c) - 1) \Delta E = 2Mk_B T(p_c) \ln 2 + 2LR_0 \varepsilon_m N^2, \quad (11)$$

where the temperature dependence is evaluated via the inversion of the thermal noise model,  $k_B T(p_c) \approx -4J/\ln(p_c)$ . This critical point satisfies  $p_c > p_{\text{th}}$ : the thermodynamic and topological thresholds are physically distinct, as we confirm numerically below. This horizon scales as  $N_{\text{max}} \propto \sqrt{\Delta E/\varepsilon_m}$ : a stronger battery or cheaper measurements extend the range, but the quadratic penalty cannot be circumvented by any improvement to the code or the decoder.

*Results and Discussion*— All simulations use STIM [24] with circuit-level noise: depolarising at rate  $p$  on all Clifford gates and bit-flip at  $p/10$  on measurements, decoded by PYMATCHING [23]. The central physical question is whether topological order can stabilise a thermodynamic resource against thermal noise well enough to make non-local work extraction profitable. Fig. 2 answers this affirmatively below  $p_{\text{th}} \approx 0.013$ . The logical error rate is exponentially suppressed,  $P_{\text{log}} \propto (p/p_{\text{th}})^{(L+1)/2}$ , so increasing  $L$  converts physical qubits directly into recoverable ergotropy with no saturation. This exponential leverage is the defining feature of topological protection and the reason the demon outperforms any finite-range entanglement-based protocol. The resource grows with system size rather than decaying with distance. Above threshold, the anyonic bath overwhelms the decoder and

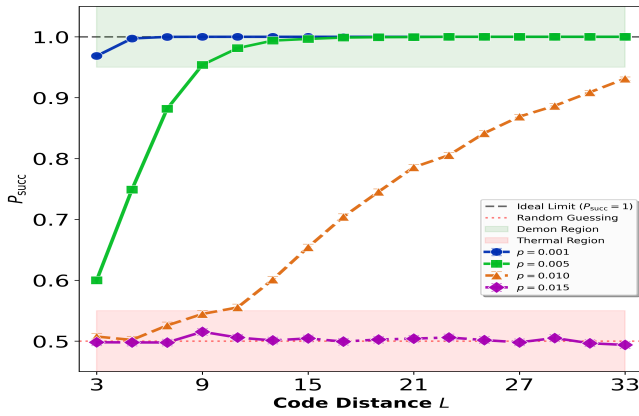


FIG. 2. Topological protection of ergotropy transfer. Decoding success probability  $P_{\text{succ}}$  versus code distance  $L$  at fixed separation  $N = 310$  for four error rates. Below  $p_{\text{th}} \approx 0.013$  (sub-threshold curves, blue, green, and orange),  $P_{\text{succ}} \rightarrow 1$  exponentially with  $L$ , demonstrating that topological protection converts physical qubits directly into recoverable ergotropy. Above threshold ( $p = 0.015$ , pink),  $P_{\text{succ}} \rightarrow \frac{1}{2}$  for all  $L$ : the battery is driven to its passive state and no ergotropy is extractable. Green (red) band: demon (thermal) phase. Solid curves: STIM Monte Carlo, 8000 shots per point.

$P_{\text{succ}} \rightarrow \frac{1}{2}$  for all  $L$ , recovering the passive-state limit  $\mathcal{E}_B = 0$ . This is precisely the condition under which no unitary can extract work, consistent with the second law. The scaling  $P_{\text{log}} \propto (p/p_{\text{th}})^{(L+1)/2}$  is consistent with Eq. (4) at fixed  $N$  and confirms that topological protection, not decoder quality, is the operative thermodynamic resource.

Figure 3 reveals richer structure. The system undergoes a continuous thermodynamic phase transition at  $p_c \approx 0.014$ , which exceeds  $p_{\text{th}}$ . The separation  $p_c > p_{\text{th}}$  is physically significant and not obvious *a priori*. The topological threshold  $p_{\text{th}}$  marks where the code ceases to protect quantum information. The thermodynamic threshold  $p_c$  marks where the cost of that protection exceeds its yield. These thresholds address physically distinct questions. The topological threshold belongs to quantum information theory. The thermodynamic threshold belongs to thermodynamics. Our protocol is the first setting in which both appear simultaneously and are measurably separated. The transition is continuous because  $P_{\text{succ}}(p)$  is smooth. There is no latent heat and no discontinuity in  $W_{\text{net}}$ , consistent with a second-order phase transition driven by the percolation of the spacetime decoding graph [17]. The quadratic scaling  $W_{\text{bulk}} \propto N^{2.05 \pm 0.04}$  is confirmed numerically in Sec. V of the Supplemental Material, together with the global phase diagram  $W_{\text{net}}(p, f)$ . This scaling is not a technical artefact but a fundamental consequence of causality. The  $R \propto N$  syndrome rounds are irreducible, and the spacetime volume of the channel grows as  $N^2$ . The resulting thermodynamic horizon  $N_{\text{max}} \approx 78$  cannot be circumvented by any improvement to the code, the decoder, or the error rate; only the ratio

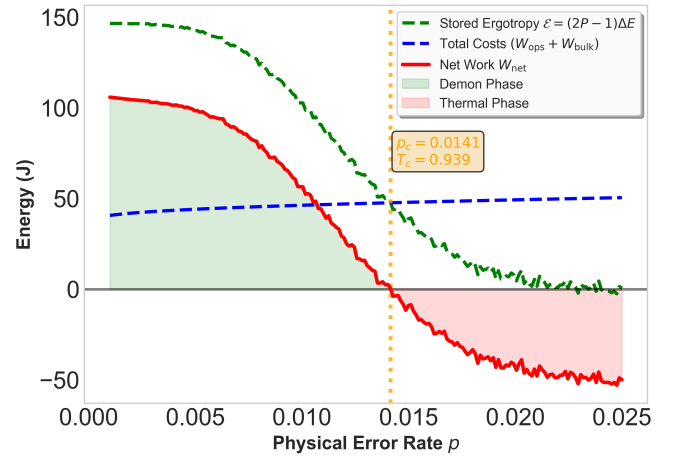


FIG. 3. Thermodynamic phase transition at  $L = 7$ ,  $N = 40$ ,  $\Delta E = 146.5$  J. Stored ergotropy  $\mathcal{E}_B = (2P_{\text{succ}} - 1)\Delta E$  (green dashed), total costs  $W_{\text{ops}} + W_{\text{bulk}}$  (blue dashed), and net work  $W_{\text{net}}$  (red solid) as functions of the physical error rate  $p$ . The demon phase ( $W_{\text{net}} > 0$ , green shading) and thermal phase ( $W_{\text{net}} < 0$ , red shading) are separated by the thermodynamic critical error rate  $p_c \approx 0.014$  (vertical dotted line), which exceeds the topological threshold  $p_{\text{th}} \approx 0.013$ . The two phase boundaries are physically distinct. The transition is continuous, reflecting the smooth degradation of  $P_{\text{succ}}(p)$  with increasing temperature. Each point: 8000 Monte Carlo shots.

$\Delta E/\varepsilon_m$  determines how far ergotropy can be teleported. Quantum energy teleportation [8, 11] transfers bare energy through a thermally fragile entangled ground state. Our protocol transfers ergotropy, the maximum work extractable by unitary operations, through a thermally robust topological structure. A state can carry high average energy yet remain thermodynamically passive and useless for any work-extraction task; ergotropy quantifies only the extractable fraction. The formal element-by-element isomorphism with QET, including the proof that both protocols are strictly LOCC, is given in Sec. VI of the Supplemental Material.

The passive decoherence instability of two-dimensional topological order [17] is not merely a theoretical concern. It is the reason the demon requires active syndrome measurement and why the infrastructure cost  $W_{\text{bulk}}$  is irreducible. Without monitoring, anyons created by thermal fluctuations diffuse freely and accumulate into logical errors on a timescale  $\tau_{\text{passive}} \sim \text{const}(T)$  independent of  $N$ . Doubling the channel length does not increase the storage time. This distinguishes topological order from an ordered ferromagnet, where the lifetime grows exponentially with system size below  $T_c$ . Figure 4 makes this quantitative. Without correction (gray), the ergotropy decays exponentially and reaches zero within  $\sim 30$  syndrome rounds. With active monitoring (orange),  $\mathcal{E}_B$  remains near  $\Delta E$  over 80 rounds because each syndrome cycle detects and removes anyons before they accumulate into a logical error. The shaded area between the two curves is the ergotropy that would be lost without

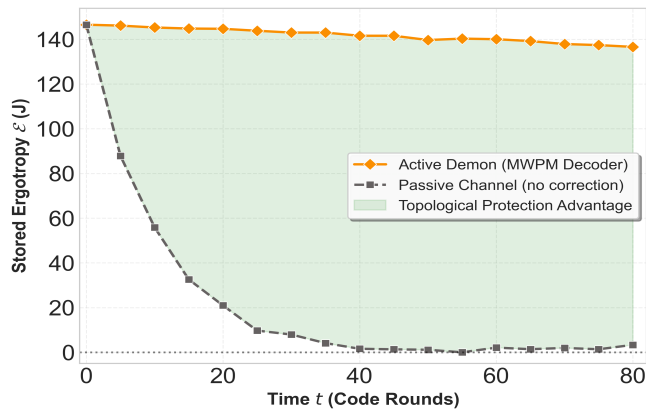


FIG. 4. Ergotropy versus syndrome rounds at  $L = 7$ ,  $N = 40$ ,  $p = 0.005$ . Without error correction (gray dashed), the ergotropy decays exponentially on a timescale independent of  $N$ , reflecting the entropic instability of two-dimensional topological order at any  $T > 0$  [17]. With active monitoring (orange), the demon sustains  $\mathcal{E}_B$  near  $\Delta E$  over 80 rounds. The shaded area quantifies the ergotropy recovered by continuous operation. It represents the thermodynamic value of the information extracted per syndrome round. Each point: 8000 shots.

continuous operation. This quantity is the thermodynamic value of the information extracted per syndrome round. Profitable operation requires that  $W_{\text{ops}}$  remain below this value.

*Conclusion.*— We have introduced and analysed a nonlocal Maxwell demon that teleports ergotropy between spatially separated parties using only classical communication and a shared topologically ordered surface code. Three results distinguish this protocol from all prior realisations of information-to-work conversion. First, topological protection provides exponential lever-

age. Increasing the code distance suppresses logical errors exponentially below the threshold, converting physical qubits directly into recoverable ergotropy without saturation. Second, the protocol exhibits a genuine thermodynamic phase transition at a critical error rate that exceeds the topological threshold. The thermodynamic and information-theoretic phase boundaries are physically distinct and simultaneously measurable. Third, causality imposes an irreducible quadratic infrastructure cost. This cost strictly enforces the second law at all separations and defines a fundamental thermodynamic horizon beyond which profitable operation is impossible, independent of code distance, decoder quality, or error rate.

These results reposition quantum error correction as a resource for thermodynamic operations, not merely for fault-tolerant computation. The protocol is compatible with current superconducting hardware, where physical error rates already approach the sub-threshold regime. Natural extensions include multi-party ergotropy distribution networks [25], the role of decoder complexity in the thermodynamic budget, and whether analogous horizons arise in other topologically ordered phases. More broadly, our work suggests that the thermodynamic cost of sustaining quantum correlations across space is not an engineering obstacle but a fundamental quantity with the same standing as Landauer’s erasure bound.

## ACKNOWLEDGMENTS

This work was supported in part by the National Key Research and Development Program of China under Contracts No. 2025YFA1613900, and by the National Natural Science Foundation of China (NSFC) under the Grants 12475087 and 12235008.

- 
- [1] R. Landauer, Irreversibility and heat generation in the computing process, *IBM Journal of Research and Development* **5**, 183 (1961).
  - [2] C. H. Bennett, The thermodynamics of computation: a review, *International Journal of Theoretical Physics* **21**, 905 (1982).
  - [3] H. S. Leff and A. F. Rex, *Maxwell’s Demon 2: Entropy, Classical and Quantum Information, Computing* (CRC Press, Boca Raton, 2003).
  - [4] A. Bérut, A. Arakelyan, A. Petrosyan, S. Ciliberto, R. Dillenschneider, and E. Lutz, Experimental verification of Landauer’s principle linking information and thermodynamics, *Nature* **483**, 187 (2012).
  - [5] J. V. Koski, V. F. Maisi, J. P. Pekola, and D. V. Averin, Experimental realization of a Szilard engine with a single electron, *Proceedings of the National Academy of Sciences USA* **111**, 13786 (2014).
  - [6] S. Toyabe, T. Sagawa, M. Ueda, E. Muneyuki, and M. Sano, Experimental demonstration of information-to-energy conversion and validation of the generalized Jarzynski equality, *Nature Physics* **6**, 988 (2010).
  - [7] T. Sagawa and M. Ueda, Generalized Jarzynski equality under nonequilibrium feedback control, *Physical Review Letters* **104**, 090602 (2010).
  - [8] M. Hotta, A protocol for quantum energy distribution, *Physics Letters A* **372**, 5671 (2008).
  - [9] M. Hotta, Quantum energy teleportation in spin chain systems, *Journal of the Physical Society of Japan* **78**, 034001 (2009).
  - [10] K. Ikeda, Demonstration of quantum energy teleportation on superconducting quantum hardware, *Physical Review Applied* **20**, 024051 (2023).
  - [11] K. Ikeda, Long-range quantum energy teleportation and distribution on a hyperbolic quantum network, *IET Quantum Communication* **5**, 543 (2024).
  - [12] A. E. Allahverdyan, R. Balian, and T. M. Nieuwenhuizen, Maximal work extraction from finite quantum systems, *Europhysics Letters* **67**, 565 (2004).

- [13] R. Alicki and M. Fannes, Entanglement boost for extractable work from ensembles of quantum batteries, *Physical Review E* **87**, 042123 (2013).
- [14] F. Campaioli, F. A. Pollock, F. Barra, L. C. Céleri, J. Goold, K. Modi, and S. Vinjanampathy, Enhancing the charging power of quantum batteries, *Physical Review Letters* **118**, 150601 (2017).
- [15] D. Ferraro, F. Campaioli, M. Cataldo, G. M. Andolina, V. Pellegrini, and M. Polini, High-power collective charging of a solid-state quantum battery, *Physical Review Letters* **120**, 117702 (2018).
- [16] A. Y. Kitaev, Fault-tolerant quantum computation by anyons, *Annals of Physics* **303**, 2 (2003).
- [17] E. Dennis, A. Kitaev, A. Landahl, and J. Preskill, Topological quantum memory, *Journal of Mathematical Physics* **43**, 4452 (2002).
- [18] A. G. Fowler, J. M. Martinis, A. C. Whiteside, and L. C. L. Hollenberg, Surface codes: towards practical large-scale quantum computation, *Physical Review A* **86**, 032324 (2012).
- [19] Google Quantum AI, Suppressing quantum errors by scaling a surface code logical qubit, *Nature* **614**, 676 (2023).
- [20] R. Acharya *et al.*, Quantum error correction below the surface code threshold, *Nature* **638**, 920 (2025).
- [21] T. He *et al.*, Experimental quantum error correction below the surface code threshold via all-microwave leakage suppression, *Physical Review Letters* **135**, 260601 (2025).
- [22] Y. Zou *et al.*, Teleportation transition of surface codes on a superconducting quantum processor 10.48550/arXiv.2602.21293 (2026).
- [23] O. Higgott and C. Gidney, Sparse Blossom: correcting a million errors per core second with minimum-weight matching, *Quantum* **9**, 1600 (2025).
- [24] C. Gidney, Stim: a fast stabilizer circuit simulator, *Quantum* **5**, 497 (2021).
- [25] M. Y. Abd-Rabbou, I. Siddique, S. Haddadi, and C.-F. Qiao, Scalable repeater architecture for long-range quantum energy teleportation in gapped systems (2026), arXiv:2601.18327v1, arXiv:2601.18327.

## Supplemental Material

Nonlocal Topological Maxwell Demon Teleporting Ergotropy via Surface-Code Quantum Error Correction

### I. LATTICE GEOMETRY AND PATH INDEPENDENCE OF $\bar{Z}_L$

The lattice  $\Lambda = \{(x, y) \in \mathbb{Z}^2 \mid 0 \leq x \leq N, 0 \leq y \leq L\}$  has horizontal edges  $(x, y) \rightarrow (x+1, y)$  and vertical edges  $(x, y) \rightarrow (x, y+1)$ . Counting gives

$$|E| = N(L+1) + (N+1)L = 2NL + N + L, \quad (\text{SM-1})$$

with  $|V| = (N+1)(L+1)$  vertices and  $|P| = NL$  plaquettes. The stabiliser group  $\mathcal{S} = \langle A_v, B_p \rangle$  has  $|V| + |P| - 2$  independent generators, arising from two linear dependencies: the X-type identity  $\prod_v A_v = \mathbf{1}$  (each edge appears in exactly two star operators) and a Z-type identity  $\prod_p B_p = \mathbf{1}$  (each interior edge appears in exactly two plaquettes, and the remaining boundary contributions cancel by the planarity of  $\Lambda$ ). The code-space dimension is therefore

$$\dim \mathcal{C} = 2^{|E| - (|V| + |P| - 2)}. \quad (\text{SM-2})$$

Euler's formula for the connected planar graph  $\Lambda$ , with  $|V|$  vertices,  $|E|$  edges, and  $|P| + 1$  faces (including the unbounded exterior face), gives

$$|V| - |E| + (|P| + 1) = 2 \implies |E| - |V| - |P| = -1. \quad (\text{SM-3})$$

Substituting into Eq. (SM-2),

$$\dim \mathcal{C} = 2, \quad (\text{SM-4})$$

encoding exactly one logical qubit, consistent with Refs. [17, 18].

Note also that the numerics use the *rotated* surface code (`surface_code_rotated_memory_z` in STIM), which places data qubits on vertices of a rotated lattice rather than on edges; the logical-qubit count and the path independence of  $\bar{Z}_L$  carry over unchanged [18].

*Path independence of  $\bar{Z}_L$ .* Let  $\gamma_1, \gamma_2$  be two horizontal paths connecting  $x = 0$  to  $x = N$ , and let  $\mathcal{R}$  be the region between them. Each interior edge of  $\mathcal{R}$  appears in exactly two plaquettes in  $\mathcal{R}$ , so

$$\prod_{p \in \mathcal{R}} B_p = \prod_{j \in \gamma_1} \sigma_j^z \cdot \prod_{j \in \gamma_2} \sigma_j^z = \bar{Z}_{\gamma_1} \bar{Z}_{\gamma_2}. \quad (\text{SM-5})$$

Since  $B_p |\psi\rangle = +|\psi\rangle$  for all  $p$  and all code states  $|\psi\rangle \in \mathcal{C}$ , Eq. (SM-5) gives  $\bar{Z}_{\gamma_1} |\psi\rangle = \bar{Z}_{\gamma_2} |\psi\rangle$ . Because of this property, Alice can exclusively apply the representative of  $\bar{Z}_L$  that is strictly confined to her  $x = 0$  boundary. This ensures her operations never interact with the bulk or Bob's side, strictly satisfying the LOCC constraints.  $\square$

### II. DERIVATION OF THE $\pi/2$ -PULSE CONDITION AND STAGE-1 DENSITY MATRIX EVOLUTION

The charging interaction is  $H_{\text{int}}(t) = g(t) \sigma_A^x \otimes \bar{Z}_L$ . In the product basis  $\{|e\rangle_A, |g\rangle_A\} \otimes \{|\bar{0}\rangle_L, |\bar{1}\rangle_L\}$ ,  $\sigma_A^x$  flips the battery and  $\bar{Z}_L$  contributes a sign. The time-evolution operator is

$$U_{\text{charge}} = \exp(-i\Phi \sigma_A^x \otimes \bar{Z}_L) = \cos \Phi \mathbf{1} - i \sin \Phi \sigma_A^x \otimes \bar{Z}_L, \quad (\text{SM-6})$$

where  $\Phi = \int_0^{\tau_1} g(t) dt$ . Setting  $\Phi = \pi/2$

$$U_{\text{charge}} |_{\Phi=\pi/2} |e\rangle_A |\bar{0}\rangle_L = -i |g\rangle_A |\bar{0}\rangle_L, \quad (\text{SM-7})$$

$$U_{\text{charge}} |_{\Phi=\pi/2} |e\rangle_A |\bar{1}\rangle_L = +i |g\rangle_A |\bar{1}\rangle_L, \quad (\text{SM-8})$$

so Alice's battery transitions  $|e\rangle_A \rightarrow |g\rangle_A$  regardless of the logical state. The pulse-area condition is therefore

$$\int_0^{\tau_1} g(t) dt = \frac{\pi}{2}. \quad (\text{SM-9})$$

*Density matrix evolution.* The code is initially prepared in a known pure logical state  $|\bar{0}\rangle\langle\bar{0}|_L$ , while the physical syndrome sector acts as a thermal bath at temperature  $T$ . Active monitoring then maintains this logical state against thermal errors, consistent with our numerical simulations. Thus, the effective initial state is  $\rho_{\text{tot}}^{(0)} = |e\rangle\langle e|_A \otimes (|\bar{0}\rangle\langle\bar{0}|_L \otimes \rho_{\text{bath}}(T)) \otimes |g\rangle\langle g|_B$ . After  $U_{\text{charge}}$  with  $\Phi = \pi/2$ , using  $U_{\text{charge}} = -i\sigma_A^x \otimes \bar{Z}_L$  and the cyclic property of the trace, tracing over the code

$$\begin{aligned} \rho_A^{(1)} &= \text{Tr}_{\text{code}} \left[ U_{\text{charge}} \left( |e\rangle\langle e|_A \otimes (|\bar{0}\rangle\langle\bar{0}|_L \otimes \rho_{\text{bath}}) \right) U_{\text{charge}}^\dagger \right] \\ &= (\sigma_A^x |e\rangle\langle e|_A \sigma_A^x) \otimes \text{Tr}_{\text{code}} \left[ \bar{Z}_L (|\bar{0}\rangle\langle\bar{0}|_L \otimes \rho_{\text{bath}}) \bar{Z}_L^\dagger \right] \\ &= \sigma_A^x |e\rangle\langle e|_A \sigma_A^x \cdot \text{Tr}_{\text{code}} [|\bar{0}\rangle\langle\bar{0}|_L \otimes \rho_{\text{bath}}] \\ &= \sigma_A^x |e\rangle\langle e|_A \sigma_A^x \\ &= |g\rangle\langle g|_A, \end{aligned} \tag{SM-10}$$

where the third line uses  $[\bar{Z}_L, H_{\text{SC}}] = 0$  (since  $\bar{Z}_L$  is a logical operator of  $\mathcal{S}$ ), which implies  $[\bar{Z}_L, \rho_{\text{th}}] = 0$  and hence  $\bar{Z}_L \rho_{\text{th}} \bar{Z}_L = \rho_{\text{th}} \bar{Z}_L^2 = \rho_{\text{th}}$ . Alice's battery is fully depleted,  $\mathcal{E}(\rho_A^{(1)}, H_A) = 0$ . Because  $[\bar{Z}_L, H_{\text{SC}}] = 0$ , the code stabiliser energy is unchanged by  $U_{\text{charge}}$ ; the energy  $\Delta E$  is expended by the external drive  $g(t)$  to encode a logical state accessible to Bob's decoder, not stored as excitation energy of  $H_{\text{SC}}$ . The energy balance is exact

$$\Delta\langle H_A \rangle_1 = -\frac{\Delta E}{2} - \frac{\Delta E}{2} = -\Delta E. \tag{SM-11}$$

### III. ERGOTROPY OF BOB'S BATTERY: COMPLETE DERIVATION

After Stage 5 of the protocol, Bob's battery is in the state

$$\rho_B^{(f)} = P_{\text{succ}} |e\rangle\langle e|_B + (1 - P_{\text{succ}}) |g\rangle\langle g|_B, \tag{SM-12}$$

with  $H_B = (\Delta E/2)\sigma_B^z$ , eigenvalues  $\varepsilon_1 = -\Delta E/2 \leq \varepsilon_2 = +\Delta E/2$ . The state is diagonal because the correction  $U_B(m) = \sigma_B^x$  is conditioned on the classical bit  $m \in \{+1, -1\}$ ; averaging over  $m$  eliminates all off-diagonal coherences, leaving a classical mixture parameterised solely by  $P_{\text{succ}}$ .

*Step 1 — Average energy.*

$$\text{Tr}(H_B \rho_B^{(f)}) = \left( P_{\text{succ}} - \frac{1}{2} \right) \Delta E. \tag{SM-13}$$

*Step 2 — Passive state.* The eigenvalues of  $\rho_B^{(f)}$  are  $r_1 = P_{\text{succ}} \geq r_2 = 1 - P_{\text{succ}}$  (assuming  $P_{\text{succ}} \geq \frac{1}{2}$ ; below this bound the state is already passive and  $\mathcal{E}_B = 0$ ). By the rearrangement inequality [12], the minimum of  $\text{Tr}(H_B U \rho_B^{(f)} U^\dagger)$  over all unitaries  $U$  is achieved by assigning the larger eigenvalue  $r_1$  to the lower energy level  $\varepsilon_1$

$$\rho_B^{\text{pass}} = P_{\text{succ}} |g\rangle\langle g|_B + (1 - P_{\text{succ}}) |e\rangle\langle e|_B. \tag{SM-14}$$

*Step 3 — Passive-state energy.*

$$\text{Tr}(H_B \rho_B^{\text{pass}}) = \left( \frac{1}{2} - P_{\text{succ}} \right) \Delta E. \tag{SM-15}$$

*Step 4 — Ergotropy.*

$$\begin{aligned} \mathcal{E}_B &= \text{Tr}(H_B \rho_B^{(f)}) - \text{Tr}(H_B \rho_B^{\text{pass}}) \\ &= \left( P_{\text{succ}} - \frac{1}{2} \right) \Delta E - \left( \frac{1}{2} - P_{\text{succ}} \right) \Delta E \\ &= (2P_{\text{succ}} - 1) \Delta E. \end{aligned} \tag{SM-16}$$

Combining both cases

$$\mathcal{E}_B = \max(0, (2P_{\text{succ}} - 1) \Delta E), \tag{SM-17}$$

which vanishes identically whenever decoding performs no better than random guessing.

The two limiting cases verify consistency:  $P_{\text{succ}} = \frac{1}{2}$  gives  $\mathcal{E}_B = 0$  (maximally mixed, thermodynamically passive);  $P_{\text{succ}} = 1$  gives  $\mathcal{E}_B = \Delta E$  (pure excited state, all energy is ergotropy).  $\square$

#### IV. SECOND LAW: COMPLETE ENTROPY PRODUCTION PROOF

We account for every entropy change over one complete cycle (Stages 1–5 plus a thermalisation step in which the surface code re-equilibrates to  $\rho_{\text{th}}(T)$  and the syndrome registers are erased at Landauer cost  $W_{\text{ops}}$ ). The surface code returns to  $\rho_{\text{th}}(T)$  after thermalisation, so  $\Delta S_{\text{sys}} = 0$ . The syndrome registers return to blank after Landauer erasure, so  $\Delta S_{\text{demon}} = 0$ . Alice’s battery starts and ends in a pure state, so  $\Delta S_{\text{batt-A}} = 0$ . Bob’s battery acquires entropy

$$\Delta S_{\text{batt-B}} = -P_{\text{succ}} \ln P_{\text{succ}} - (1 - P_{\text{succ}}) \ln(1 - P_{\text{succ}}) \geq 0. \quad (\text{SM-18})$$

The costs  $W_{\text{ops}}$  and  $W_{\text{bulk}}$  are paid by external work reservoirs (the erasure apparatus and the measurement apparatus, respectively); they are not drawn from Alice’s battery  $\Delta E$ . Under this accounting, the total energy entering the thermal bath is

$$Q_{\text{bath}} = \Delta E + W_{\text{ops}} + W_{\text{bulk}} - \mathcal{E}_B, \quad (\text{SM-19})$$

giving  $\Delta S_{\text{bath}} = Q_{\text{bath}}/T$ . The total entropy production is therefore

$$\Delta S_{\text{total}} = \Delta S_{\text{batt-B}} + \frac{Q_{\text{bath}}}{T}. \quad (\text{SM-20})$$

The Sagawa-Ueda bound [7] gives

$$\mathcal{E}_B \leq k_B T I(E : \vec{s}_A) \leq k_B T M \ln 2 \leq W_{\text{ops}}, \quad (\text{SM-21})$$

where the second inequality bounds the mutual information by the Shannon entropy of  $M$  binary bits, and the third uses  $W_{\text{ops}} = 2Mk_B T \ln 2 \geq Mk_B T \ln 2$ . Substituting into Eq. (SM-19)

$$Q_{\text{bath}} = \Delta E + W_{\text{ops}} + W_{\text{bulk}} - \mathcal{E}_B \geq \Delta E + W_{\text{bulk}} > W_{\text{bulk}} > 0, \quad (\text{SM-22})$$

so  $\Delta S_{\text{bath}} \geq W_{\text{bulk}}/T$ . Since  $\Delta S_{\text{batt-B}} \geq 0$ :

$$\Delta S_{\text{total}} \geq \frac{W_{\text{bulk}}}{T} = \frac{2R_0 \varepsilon_m N^2}{T} > 0 \quad (\text{SM-23})$$

for all  $N > 0$ , regardless of  $P_{\text{succ}}$ ,  $L$ , or  $p$ . □

#### V. EXTENDED NUMERICAL RESULTS

*Information threshold and percolation.* Alice’s syndrome  $\vec{s}_A$  is not merely a label for Bob’s operation. It is the physical mechanism by which thermal noise is rectified into directed ergotropy flow. Figure SM-1 quantifies this by varying the information fraction  $f$ , the proportion of Alice’s  $M$  boundary syndromes transmitted to Bob. Below  $f_c \approx 0.62$ , the decoding graph lacks a spanning connected cluster: Bob cannot distinguish the true error chain from its complement, and  $P_{\text{succ}} \rightarrow \frac{1}{2}$  regardless of code distance or error rate. This is a bond percolation transition in the  $(2+1)$ -dimensional spacetime decoding graph; the super-linear onset  $\mathcal{E}_B \propto f^\alpha$  with  $\alpha = 2.7 \pm 0.1$  reflects the critical scaling near the percolation threshold, where the connected cluster grows faster than linearly with bond occupation probability. The operational cost  $W_{\text{ops}}$  grows only linearly with  $f$ , so below  $f_c$  the demon pays Landauer’s cost for information it cannot use, and  $W_{\text{net}} < 0$ . This establishes a minimum information requirement that is independent of both code distance and error rate. Even a perfect decoder operating on a perfect code cannot extract ergotropy without a minimum density of classical syndrome information.

*Quadratic scaling and thermodynamic horizon.* The  $N^2$  growth of  $W_{\text{bulk}}$  is a consequence of special relativity applied to quantum error correction: Alice’s syndrome at  $x = 0$  cannot reach Bob at  $x = N$  in fewer than  $N/c_{\text{signal}}$  time steps, so a minimum of  $R \propto N$  syndrome rounds must be completed before decoding. The maintained spacetime volume is  $N \times R \propto N^2$ , and each unit costs  $\varepsilon_m$  to monitor. This is not an engineering limitation. No improvement in qubit quality, gate speed, or decoder efficiency can remove the  $N^2$  factor, because its origin is kinematic. Figure SM-2 confirms  $\beta = 2.05 \pm 0.04$ , indistinguishable from 2 within statistical uncertainty, and shows the resulting parabolic profile of  $W_{\text{net}}(N)$  crossing zero at  $N_{\text{max}} \approx 78$ . The ergotropy  $\mathcal{E}_B$  is nearly flat with  $N$  (less than 5% variation over the full range), so the horizon is set entirely by the intersection of a constant and a parabola: a clean geometric consequence of the competition between a topologically protected resource and a causally enforced cost.

*Global phase diagram.* The phase diagram  $W_{\text{net}}(p, f)$  in Figure SM-3 unifies all three thresholds (topological  $p_{\text{th}}$ , thermodynamic  $p_c$ , and information  $f_c$ ) into a single operational map. The demon phase occupies the low- $p$ , high- $f$

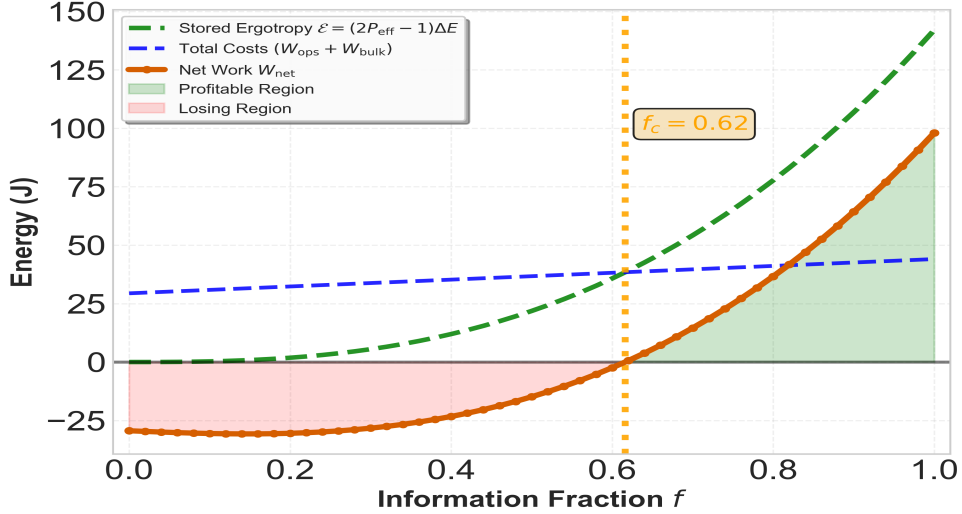


FIG. SM-1. Information threshold for thermodynamic profit at  $L = 7$ ,  $N = 40$ ,  $p = 0.005$ . Below the critical fraction  $f_c \approx 0.62$  (vertical dotted line), the syndrome record is too sparse to span the decoding graph: Bob cannot distinguish the logical error class and  $\mathcal{E}_B \rightarrow 0$ . The super-linear onset  $\mathcal{E}_B \propto f^{2.7}$  is a percolation critical exponent, not a property of the decoder. Solid curve: percolation model  $P_{\text{eff}}(f) = \frac{1}{2} + (P_{\text{raw,full}} - \frac{1}{2})f^\alpha$  with  $\alpha = 2.7 \pm 0.1$  from percolation universality and  $P_{\text{raw,full}}$  measured from a single STIM simulation at  $f = 1$  (8000 shots); the  $f$ -dimension is computed analytically from the model.

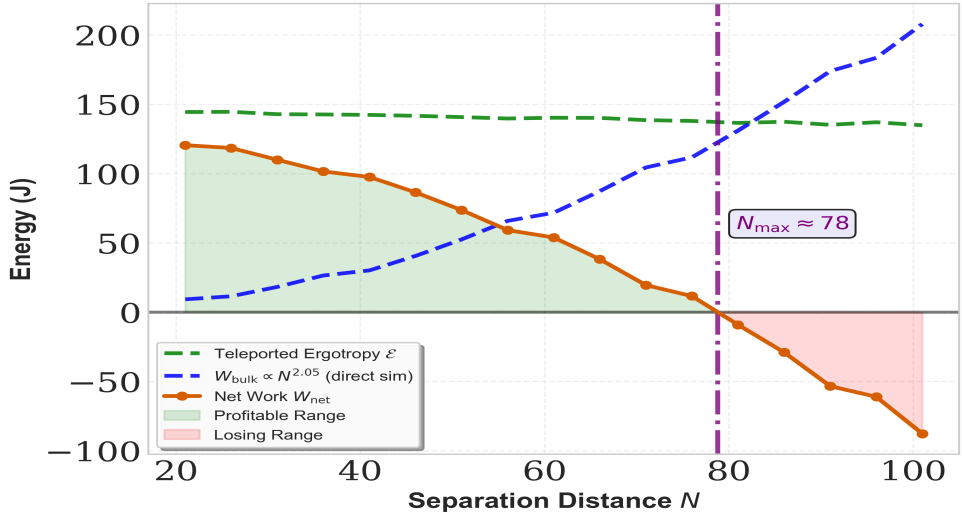


FIG. SM-2. Energy-distance trade-off at  $L = 7$ ,  $p = 0.005$ . The ergotropy  $\mathcal{E}_B$  (green dashed) is nearly constant with  $N$  because exponential topological suppression makes the distance correction negligible at sub-threshold error rates. The infrastructure cost  $W_{\text{bulk}}$  (blue dashed) grows as  $N^{2.05 \pm 0.04}$ , confirming the causal  $N^2$  prediction. Net work  $W_{\text{net}}$  (red solid) follows a parabola and crosses zero at the thermodynamic horizon  $N_{\text{max}} \approx 78$ . Each point: 8000 STIM shots.

corner, where topological protection is strong and the syndrome record is dense enough to span the decoding graph. The break-even contour  $f_c(p)$  rises steeply as  $p \rightarrow p_{\text{th}}$ . Near the topological threshold, the ergotropy per syndrome bit collapses and the demon must use nearly all of Alice's record to remain profitable. This steep rise is the thermodynamic signature of the topological phase transition. It diverges precisely at  $p_{\text{th}}$  in the limit  $L \rightarrow \infty$ , where the code distance scaling becomes exact. The demon phase occupies approximately 20% of the  $(p, f)$  parameter space, a stringent but achievable operating window given current superconducting qubit error rates of  $p \approx 0.003$  and classical communication efficiencies exceeding  $f = 0.9$ .

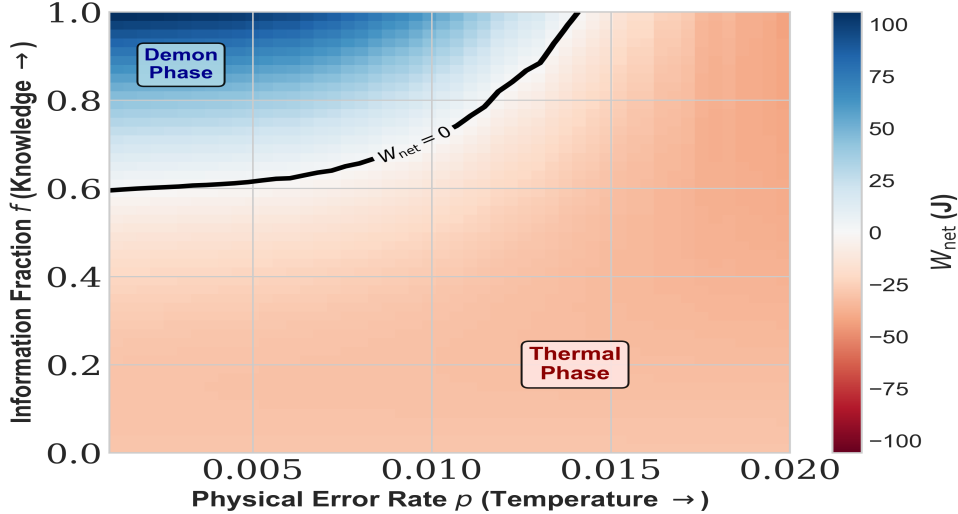


FIG. SM-3. Global operational phase diagram  $W_{\text{net}}(p, f)$  at  $L = 7$ ,  $N = 40$ . Blue: demon phase; red: thermal phase. Black contour: break-even boundary  $f_c(p)$ . The steep rise of  $f_c(p)$  as  $p \rightarrow p_{\text{th}}$  is the thermodynamic signature of the topological phase transition: at the threshold, the demon must use the entire syndrome record to remain profitable because ergotropy per syndrome bit vanishes. The demon phase occupies  $\approx 20\%$  of parameter space, accessible with current superconducting hardware. For each value of  $p$ ,  $P_{\text{raw}}(p)$  is measured by direct STIM simulation at  $f = 1$  (8000 shots per  $p$  value); the  $f$ -dimension is computed analytically from the percolation model of Sec. V.

## VI. FORMAL ISOMORPHISM WITH QUANTUM ENERGY TELEPORTATION

Both protocols are strictly LOCC. In QET [8, 10], Alice measures her local operator  $P_0(\mu) = \frac{1}{2}(1 + \mu\sigma_0^x)$ , transmits the classical bit  $\mu$ , and Bob applies conditional unitary  $U_1(\mu)$  to extract energy  $E_B$  from the entangled ground state  $|g\rangle$ . In our protocol, Alice charges the logical qubit and measures  $M$  boundary stabilisers, transmits the classical string  $\vec{s}_A$ , and Bob applies  $U_B(m)$  to extract ergotropy  $\mathcal{E}_B$  from the topologically ordered code. The structural mapping is element-by-element, as summarised in Table SM-1.

TABLE SM-1. Formal mapping between QET and ergotropy teleportation.

Element	QET	This work
Shared resource	Entangled ground state $ g\rangle$	Topological logical qubit
Alice's operation	Measurement $P_0(\mu)$	Charge + measure $\vec{s}_A$
Classical communication	1 bit $\mu$	$M$ bits $\vec{s}_A$
Bob's operation	$U_1(\mu)$	$U_B(m)$
Transferred quantity	Energy $E_B$	Ergotropy $\mathcal{E}_B$
Thermal robustness	Fragile ( $T > 0$ degrades $ g\rangle$ )	Robust ( $p < p_{\text{th}}$ )
Distance limit	Coherence length	$N_{\text{max}}$

The key physical distinction is that QET transfers bare energy, which need not be extractable as work. A state can have high average energy yet be thermodynamically passive. Our protocol transfers ergotropy by construction, guaranteeing that the delivered quantity is operationally useful for any subsequent work-extraction task. The second distinction is thermal robustness. The entangled ground state  $|g\rangle$  is degraded at any  $T > 0$  by corrections of order  $e^{-\beta\Delta}$ , whereas topological protection suppresses logical errors exponentially in  $L$  for all  $p < p_{\text{th}}$ , making the protocol viable at experimentally accessible temperatures. A complementary approach to the range limitation of QET employs quantum-repeater architectures [25], achieving polynomial energy-cost scaling via heralded entanglement purification. Our protocol differs fundamentally: it replaces the probabilistic repeater chain with a single topologically protected channel, trading polynomial repeater overhead for the deterministic quadratic infrastructure cost  $W_{\text{bulk}} \propto N^2$ .